RNA (1998), *4*:1216–1229. Cambridge University Press. Printed in the USA.

PRP16, a DEAH-box RNA helicase, is recruited to the spliceosome primarily via its nonconserved N-terminal domain

YAN WANG and CHRISTINE GUTHRIE
Department of Biochemistry, University of California, San Francisco, California 94143-0448, USA

ABSTRACT

Dynamic rearrangement of RNA structure is crucial for intron recognition and formation of the catalytic core during pre-mRNA splicing. Three of the splicing factors that contain sequence motifs characteristic of the DExD/DExH-box family of RNA-dependent ATPases (Prp16, Prp22, and the human homologue of Brr2) recently have been shown to unwind RNA duplexes in vitro, providing biochemical evidence that they may direct structural rearrangements on the spliceosome. Notably, however, the unwinding activity of these proteins is sequence nonspecific, raising the question of how their functional specificity is determined. Because the highly conserved DExD/DExH-box domain in these proteins is typically flanked by one or more nonconserved domains, we have tested the hypothesis that the nonconserved regions of Prp16 determine the functional specificity of the protein. We found that the nonconserved N-terminal domain of Prp16 is (1) essential for viability, (2) required for the nuclear localization of Prp16, and (3) capable of binding to the spliceosome specifically at the step of Prp16 function. Moreover, this domain can interact with the rest of the protein to allow *trans*-complementation. Based on these results, we propose that the spliceosomal target of the unwinding activity of Prp16, and possibly other DExD/DExH-box splicing factors as well, is defined by factors that specifically interact with the nonconserved domains of the protein.

Keywords: deletion analyses; spliceosome binding; *trans*-complementation

INTRODUCTION

Nuclear pre-mRNA splicing is a process used by eukaryotic cells to remove the noncoding regions (introns) from the precursor mRNA to ligate the coding regions (exons) to form mature mRNA. The chemical mechanism of pre-mRNA splicing is identical to that used by the self-splicing Group II introns: first, the nucleophilic attack of the phosphate group at the 5′ splice site by the 2′ hydroxyl (OH) group of the branch point adenosine leads to the formation of a lariat intermediate and excised 5′ exon; second, nucleophilic attack of the 3′ splice site by the OH group at the 3′ end of the 5′ exon leads to cleavage at the 3′ splice site and ligation of the two exons. Although energy is not required for the two transesterification reactions, pre-mRNA splicing does require ATP hydrolysis. Unlike the Group II introns, which can self-splice in vitro, the splicing of pre-mRNA requires a large ribonucleoprotein machinery, the spliceosome, which is formed by five small nuclear RNAs (snRNAs), U1, U2, U4, U5, and U6, and more than 50 protein factors. Conserved intramolecular and intermolecular base pairing interactions have been identified among the snRNAs, as well as between the snRNAs and pre-mRNA. Notably, the spliceosome is a dynamic machine, which undergoes multiple conformational rearrangements in RNA structure during the splicing pathway (Madhani & Guthrie, 1994a; Ares & Weiser, 1995; Nilsen, 1998). Although the RNA components of the spliceosome are thought to form the catalytic core of the spliceosome, an important role of the protein components is to direct RNA structural rearrangements in the spliceosome that are critical for catalysis (Guthrie, 1991; Rymond & Rosbash, 1992; Moore et al., 1993; Will & Lührmann, 1997; Staley & Guthrie, 1998).

In recent years, many pre-mRNA processing (prp) factors have been identified genetically in *Saccharomyces cerevisiae* and characterized further biochemically (Guthrie, 1991; Ruby & Abelson, 1991; Rymond & Rosbash, 1992; Staley & Guthrie, 1998). One class of factors is of particular interest in light of the requirement for ATP hydrolysis in splicing. This class of factors [Prp2, Prp5, Prp16, Prp22, Prp28, Prp43, and Brr2 (also

Reprint requests to: Christine Guthrie, Department of Biochemistry, University of California, San Francisco, California 94143-0448, USA; e-mail: guthrie@cgl.ucsf.edu.

known as Snu246, Slt22, and Rss1)] shares a highly homologous domain that was identified initially in the eukaryotic translation initiation factor eIF4A (Fig. 1) (Burgess & Guthrie, 1990; Chen & Lin, 1990; Dalbadie-McFarland & Abelson, 1990; Company et al., 1991; Strauss & Guthrie, 1991; Gorbalenya & Koonin, 1993; Lin & Rossi, 1996; Noble & Guthrie, 1996; Xu et al., 1996; Arenas & Abelson, 1997). This domain contains seven conserved signature motifs (Fig. 1). Because motif III in eIF4A is an Asp-Glu-Ala-Asp (DEAD) tetrapeptide, members of this family have been referred to as "DEAD-box" proteins, although variations in this motif as well as in the other motifs are common (Schmid & Linder, 1992; Fuller-Pace, 1994). We will refer to these proteins as DExD/DExH-box factors.

Five of the DExD/DExH-box splicing factors have been shown to be RNA-dependent or RNA-stimulated ATPases or NTPases using homopolymeric RNA as the ligand (Schwer & Guthrie, 1991; Kim et al., 1992; O'Day et al., 1996; Xu et al., 1996). Like eIF4A, three of these factors, Prp16, Prp22, and the human homologue of Brr2, can catalyze the unwinding of RNA duplexes in an ATP (or NTP)-dependent and sequence nonspecific fashion (Rozen et al., 1990; Laggerbauer et al., 1998; Schwer & Gross, 1998; Wagner et al., 1998; Wang et al., 1998). Interestingly, despite the sequence nonspecific nature of the biochemical activities (i.e., ATPase activation and duplex unwinding), these DExD/DExH-box splicing factors are required for distinct steps in splicing both in vivo and in vitro. Thus, a key question in understanding how the biochemical activities of these DExD/DExH-box splicing factors are coupled to RNA structural rearrangement is how their functional specificity is determined. Evidence from previous findings suggests that the functional specificity of these proteins may be temporally controlled by their association with the spliceosome (Schwer & Guthrie, 1991; Teigelkamp et al., 1994). Brr2, like its human counterpart, is an integral component of the U5 snRNP, which is incorporated into the spliceosome during spliceosome assembly (Lauber et al., 1996), whereas others (e.g., Prp2, Prp16, and Prp22) are *trans*-acting factors that are recruited onto the spliceosome at later steps. Prp2, required for the first step, associates specifically with spliceosomes containing pre-mRNA (Teigelkamp et al., 1994). Prp16, required for the second step, associates specifically with spliceosomes containing lariat intermediates (Schwer & Guthrie, 1991). Prp22, which has a dual function in the second step and in mRNA release, associates with spliceosomes containing either lariat intermediates or mRNA in the absence of ATP (Company et al., 1991; Schwer & Gross, 1998).

These DExD/DExH-box splicing factors are characterized by a distinct domain structure (Fig. 1). The highly conserved DExD/DExH-box domain, the so-called helicase domain (domain H in Fig. 1), is flanked by a nonconserved N-terminal domain (domain N in Fig. 1) and a C-terminal domain (domain C in Fig. 1), which is conserved only among a subset of proteins (e.g., Prp2, Prp16, Prp22, and Prp43) (Company et al., 1991; Arenas & Abelson, 1997). In Prp16 and Prp22, the nonhomologous region that is C-terminal to domain C is designated as the tail domain (domain T in Fig. 1). Previous mutagenesis and biochemical analyses have

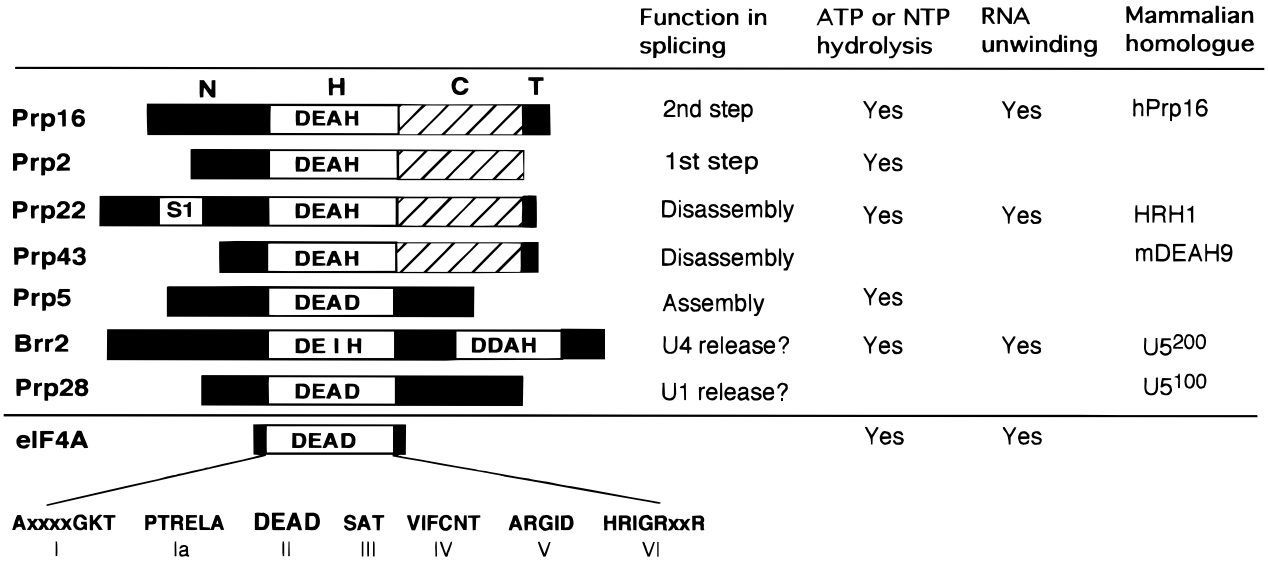

FIGURE 1. Summary of the DExD/DExH-box proteins that function in pre-mRNA splicing in *S. cerevisiae*. Schematic domain structure of each protein is shown along with that of eIF4A. Definition (N, H, C, and T) of the domains is shown at the top. Amino acid sequence of the seven conserved motifs in eIF4A is shown at the bottom. Nonconserved regions in each protein are in black, regions that are conserved among the DEAH-box splicing factors are in hash mark, and the highly conserved DExD/DExH-box domain is in white with the identity of motif II indicated. The S1 RNA binding motif in Prp22 and the second and less well-conserved helicase-like motif in Brr2 are also indicated.

established the functional importance of the H domain in ATP binding/hydrolysis, RNA binding, and duplex unwinding (Pause & Sonenberg, 1992; Pause et al., 1993; Gross & Shuman, 1995), whereas much less is known about the nonconserved regions. In light of the nonspecific nature of the biochemical activities associated with the H domain with respect to the RNA substrate, an intriguing possibility is that the nonconserved regions in these proteins are involved in specific interactions with the spliceosome.

We have focused on Prp16, which is the best-characterized DExD/DExH-box splicing factor. We have generated deletion mutants lacking single or multiple domains of Prp16. Through genetic and biochemical analyses of these mutants, we have uncovered the functional importance of the nonconserved N-terminal domain of Prp16. We show that (1) the C-terminal half of the N-terminal domain of Prp16 is essential for cell viability; (2) the N-terminal domain is required for the nuclear localization of Prp16; (3) the N-terminal domain is capable of binding to the spliceosome specifically at the step of Prp16 function; and (4) the N-terminal domain and the HCT domains can form a bipartite Prp16 to allow *trans*-complementation. Based on these findings, we propose that the spliceosomal target of the unwinding activity of Prp16 is defined by specific interactions of spliceosomal factors with the nonconserved N-terminal domains of Prp16, rather than with the conserved DExD/DExH-box domain.

RESULTS

In vivo analyses of deletion mutants

At the time this study was initiated, the minimal functional region of PRP16 in vivo had not been determined. As a single copy essential gene (Burgess & Guthrie, 1990), *PRP16* allows us to identify the regions/domains that are functionally essential in vivo by analyzing the viability of cells expressing truncated proteins as the sole source of Prp16. We have constructed three sets of deletion mutants: (1) partial or complete deletions of the N or the T domain; (2) combined deletions in both the N and the T domains; and (3) deletions of the conserved H and the C domains.

Three partial deletions were introduced in the N domain, ΔN1, ΔN2, and ΔN3, deleting the first 76, 149, and 228 amino acids, respectively. The effects of these deletions on the in vivo function of *PRP16* were determined by a plasmid shuffle assay (Sikorski & Boeke, 1991). As shown in Table 1, deletion of the N-terminal 149 amino acids (ΔN2) or the T domain (ΔT) has no effect on cell growth, suggesting that these two regions are dispensable in the context of an otherwise wild-type protein. Further deletion of the N domain (ΔN3), eliminating the first 228 amino acids, results in slower than wild-type growth of the cells at temperatures at or below 30 °C, and no growth at 37 °C. This temperature sensitive (ts)/sick phenotype is suppressed when ΔN3 is overexpressed.

Interestingly, the effects of the partial deletion in the N domain and the deletion of the T domain appear to be synergistic, because, when combined, cell growth is more severely affected. For instance, a lethal phenotype is observed when ΔN2 and ΔT are combined (ΔN2T), whereas the individual deletions are tolerated. Similarly, the combination of ΔN3 and ΔT is also lethal (see ΔN3T in Table 1). Both lethal phenotypes are suppressed or partially suppressed when the truncations are overexpressed. These results suggest that the first half of the N domain and the entire T domain are functionally nonessential or redundant. We observed no

TABLE 1. Summary of the deletion mutants of PRP16 and their growth phenotypes.

Deletion construct	Growth on 5-FOA							
	Low copy (CEN)				High copy (2 μ, GPD)			
	18	25	30	37 °C	18	25	30	37 °C
WT	++	++	++	++	++	++	++	++
ΔN1	++	++	++	++	++	++	++	++
ΔN2	++	++	++	++	++	++	++	++
ΔN3	+	+	+	−	++	++	++	++
HCT	−	−	−	−	−	−	−	−
ΔT	++	++	++	++	ND	ND	ND	ND
ΔN1T	++	++	++	++	++	++	++	++
ΔN2T	−	−	−	−	+	++	++	++
ΔN3T	−	−	−	−	−	+	+	−
NH	−	−	−	−	−	−	−	−
N	−	−	−	−	−	−	−	−
H	−	−	−	−	−	−	−	−
CT	−	−	−	−	−	−	−	−

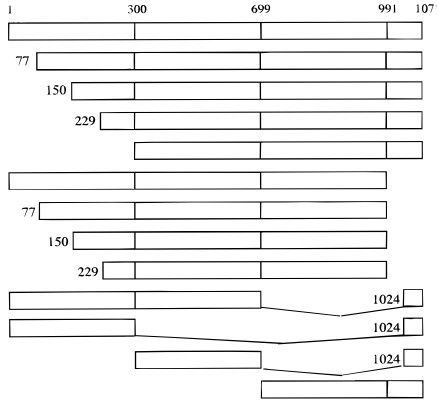

significant difference between the protein level of ΔN2 and that of ΔN2T (data not shown). Unlike the nonconserved N and T domains, deletion of the conserved domains H and C is lethal. Overexpression of these truncations does not rescue the lethal phenotype (Table 1). By western analyses, we observed stable expression of all truncations tested (data not shown), suggesting that these deletions are likely to affect Prp16 function rather than its stability.

In summary, (1) the C-terminal half of the N domain is essential for the in vivo function of Prp16; (2) the nonconserved T domain is dispensable in vivo; however, deletion of this domain is synergistic with deletion in the N domain; and (3) deletion of the H and C domains is lethal. In addition to confirming the recent report of similar deletion analyses of PRP16 (Hotz & Schwer, 1998), our results also address the effect of overexpression on the function of a number of deletion mutants of PRP16.

N domain is required for the nuclear localization of Prp16

Having demonstrated the requirement of the N domain for cell viability, we further explored the basis of this requirement. Because pre-mRNA splicing is a nuclear event, nuclear localization of Prp16 is a prerequisite for its function in splicing. Partial deletion of the N domain of HRH1, the mammalian homologue of PRP22, has been shown to change the localization pattern of the protein (Ohno & Shimura, 1996). To test whether the N domain of Prp16 is required for its proper localization, we investigated the subcellular localization of the triple hemaglutinin (HA_3)-tagged wild-type protein (Prp16-HA_3) and the truncation lacking the N domain (HCT-HA_3) by indirect immunofluorescence analysis. As shown in Figure 2, the wild-type Prp16 is localized to the nucleus (Fig. 2A,B), whereas HCT-HA_3 is clearly concentrated in the cytoplasm (Fig. 2C,D). Thus, we conclude that the N domain of Prp16 is required for the nuclear localization (or retention) of Prp16.

Interestingly, when the N domain of Prp16 is substituted by the N domain of Prp2, the chimeric protein (2N16-HA_3) is now localized to the nucleus (Fig. 2E,F). This result suggests that, similar to the N domain of Prp16, the N domain of Prp2 also determines the nuclear localization of the protein. This chimeric protein cannot functionally substitute for Prp16 in vivo (data not shown), however, suggesting that the N domain of Prp16 must play an additional role besides ensuring the nuclear localization (or retention) of the protein.

N domain of Prp16 functions as the spliceosome binding domain

As described earlier, previous studies suggest that the functional specificity of the DExD/DExH-box proteins may be temporally determined at the step of spliceosome binding. Therefore, determining the spliceosome binding domain(s) in Prp16 should provide important insight to how its functional specificity is determined. Using four of the truncations generated in the deletion analyses, N, H, NH, and HCT, we used three approaches to determine the spliceosome binding domain in Prp16.

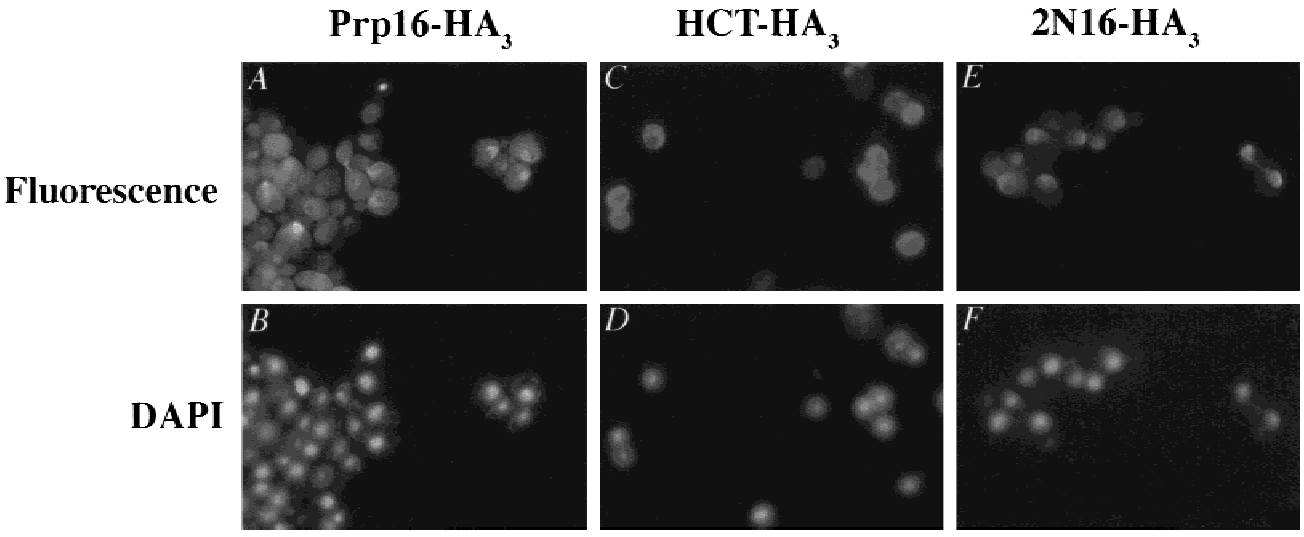

FIGURE 2. Deletion of the N domain of Prp16 causes accumulation of the truncated protein in the cytoplasm. Cells expressing Prp16-HA_3 (left), or HCT-HA_3 (middle), or 2N16-HA_3 (right) were fixed in formaldehyde before spheroplasting with zymolyase (see Materials and Methods). Binding of the fluorochrome was achieved by first incubating the fixed cells with 12CA5, which recognizes the HA epitope, and then incubating with the fluorochrome-conjugated goat-anti-mouse antibody. DAPI was included in the mounting solution. **A,C,E:** Fluorescent stain that identifies the localization of the HA_3-tagged protein. **B,D,F:** DAPI stain that identifies the position of the nucleus.

Lariat intermediates can be co-immunoprecipitated with the N domain

Prp16 associates with the spliceosome in vitro before the second step of splicing occurs. In the absence of ATP, the wild-type Prp16 associates predominantly with lariat intermediates (Schwer & Guthrie, 1991). Thus, the spliceosome binding domain of Prp16 is expected to associate with the same splicing intermediates as does the full-length protein. Each truncation was expressed under the control of the constitutively active glyceraldehyde-3-phosphate dehydrogenase (GPD) promotor in a strain in which the wild-type Prp16 contained a C-terminal HA_3 tag. Extracts were prepared from each strain, and Prp16-HA_3 was subsequently immunodepleted using the 12CA5 antibody (see Materials and Methods). Greater than 90% of the tagged Prp16 is depleted from each extract as assayed by western blot (Fig. 3, compare lanes 1, 3, 5, and 7 with lanes 2, 4, 6, and 8). We used a co-immunoprecipitation (co-IP) assay to assess the ability of each truncation to associate with the spliceosome. The experiment was performed using radiolabled pre-mRNA under two buffer conditions, one in the presence of 0.1% NP40 and the other in the absence of any detergent. Under the former and more stringent condition, co-IP of the lariat intermediate was observed only with the wild-type extract (data not shown). When no detergent was used, co-IP of the lariat intermediates was observed reproducibly in the wild-type extract (Fig. 4, lane 8) as well as in extract containing either N or NH domains (Fig. 4, lanes 9 and 12), but not in the extract containing either H or HCT domains (Fig. 4, lanes 10 and 11). As shown at the bottom of Figure 4, whereas the ratio of lariat intermediate to pre-mRNA in the splicing reaction is similar (less than 1.3-fold difference) for each sample, the same ratio taken from the co-IP samples containing the wild-type Prp16, NH, or N is significantly higher (2–4-fold) than the rest. This demonstrates that, although the efficiency of the co-IP reaction is low, the difference observed is significant quantitatively, and is specific to the lariat intermediates. The difference in co-IP efficiency is unlikely to be due to a difference in antibody binding or in the protein level of the truncated proteins, because all four truncations can be recognized by the anti-Prp16 antibodies under a nondenaturing condition (data not shown), and they are expressed at similar levels (Fig. 3).

These results lead us to two conclusions. First, the N domain alone is capable of associating with the same

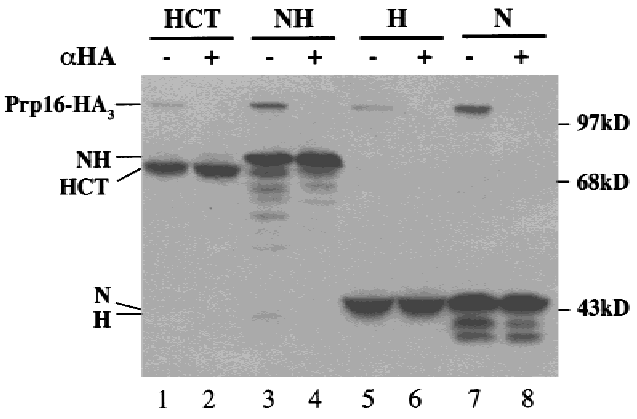

FIGURE 3. Immunodepletion of HA_3-tagged Prp16 from extract. Extract containing both Prp16-HA_3 and truncated proteins was treated with 12CA5 bound to protein-A–sepharose to remove Prp16-HA_3. The resulting supernatant was compared with the untreated extract to estimate the efficiency of depletion. Lanes 1, 3, 5, and 7, untreated extracts; lanes 2, 4, 6, and 8, 12CA5-treated extracts. Truncated proteins present in each extract are indicated above and beside the gel, and molecular weight markers are indicated at the right.

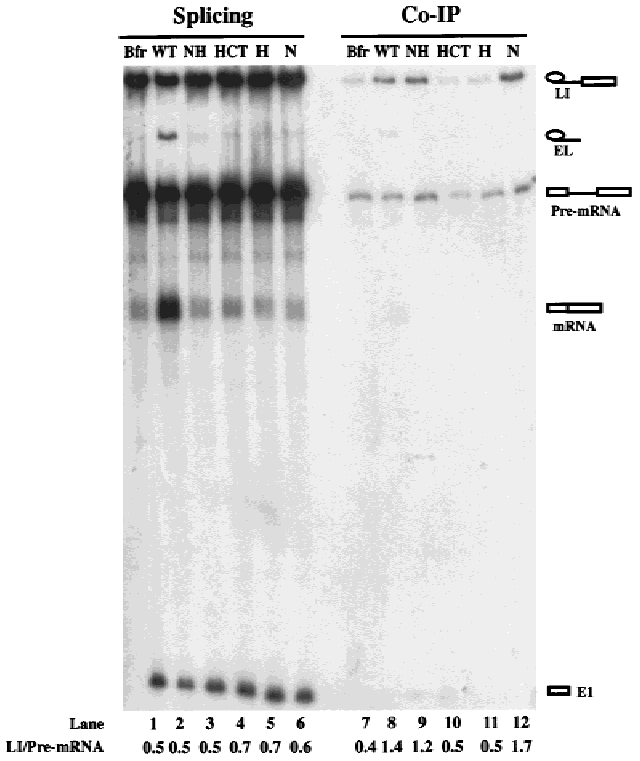

FIGURE 4. Co-immunoprecipitation of splicing intermediates with truncated Prp16. In vitro splicing reaction was initiated by the addition of 12 μL of ΔPrp16 extract to 8 μL of reaction mixture containing radiolabeled actin pre-mRNA of 1–5 fmol (3,000 cpm/fmol) and reaction buffer (Lin et al., 1985). The reaction was incubated at 25 °C for 20 min before the addition of 3 μL of the last dialysis buffer in extract preparation (lanes 1 and 7), recombinant Prp16 (lanes 2 and 8), or extract containing various truncations (NH, lanes 3 and 9; HCT, lanes 4 and 10; H, lanes 5 and 11; N, lanes 6 and 12). The mixture was allowed to incubate at 25 °C for an additional 10 min. Three microliters of the reaction was taken to be analyzed for splicing activity. Unlabeled actin pre-mRNA of 500-fold molar excess of the labeled substrate was added to the remaining reaction before the addition of the anti-Prp16 polyclonal antibodies that are bound to protein-A–sepharose and 200 μL of IPP_{150}. After a 1-h incubation with rocking at 4 °C and three washes with 200 μL of the binding buffer, the RNAs that remained bound to the beads were recovered by phenol extraction and ethanol precipitation and analyzed on a 6% denaturing polyacrylamide gel. Lanes 1–6, splicing reactions; lanes 7–12, samples from immunoprecipitation pellets. The ratio of lariat intermediate (LI) to pre-mRNA for each sample is shown at the bottom.

splicing intermediates as does the wild-type Prp16. Second, because deletion of both the C and the T domains renders the co-immunoprecipitation signal sensitive to detergent, one or both of these domains must function to stabilize the interactions between the N domain and the spliceosome. The enhancement could be due to either direct, albeit weaker, interactions between the CT domains and the spliceosome, or an indirect effect on the conformation of the N domain.

Truncations containing the N domain are dominant negative in vitro

To qualify as the spliceosome binding domain, the N domain must bind to the same site on the spliceosome as does the full-length protein. Although the profile of splicing intermediates co-immunoprecipitated by the N domain alone and by the full-length protein are identical, this does not prove that the two proteins bind to the same site on the spliceosome. If indeed it is the authentic Prp16 binding site that is recognized by the N domain alone, the presence of excess N domain should inhibit the splicing activity of the wild-type Prp16 in vitro. We prepared splicing extract from cells expressing Prp16-HA_3 and overexpressing N, H, NH, or HCT. First, we examined the splicing efficiency of these extracts. The splicing efficiency of extract containing HCT or H is very similar to that of the control extract, which contains just Prp16-HA_3 (Fig. 5, compare lanes 1, 4, and 10). On the contrary, the splicing efficiency is moderately reduced in extract containing NH (Fig. 5, lane 7), and is significantly reduced in extract containing N (Fig. 5, lane 13). This suggests that the presence of excess N or NH may inhibit the function of the wild-type Prp16, possibly by competing for the Prp16 binding site on the spliceosome.

A previous study revealed that the presence of Prp16-1 mutant protein inhibits the function of the wild-type protein in a manner that is greatly dependent on the order of addition of the two proteins to the splicing reaction (Schwer & Guthrie, 1992b); pre-binding of the mutant protein to the spliceosome results in the most pronounced inhibitory effect. To examine whether the inhibition of the wild-type Prp16 function by N and NH can be exacerbated by pre-binding the truncations to the spliceosome, we immunodepleted Prp16-HA_3 (ΔPrp16) from the above extracts, and analyzed how splicing is affected with or without the addition of purified Prp16.

Upon immunodepletion of the full-length Prp16, significant reduction in the amounts of mature mRNA was observed with each of the extracts tested (Fig. 5, lanes 2, 5, 8, 11, and 14). In addition to demonstrating that the HA_3-tagged Prp16 is removed efficiently from the extracts, this also confirms that none of these truncated proteins can substitute for the function of the wild-type Prp16 in vitro. When purified recombinant

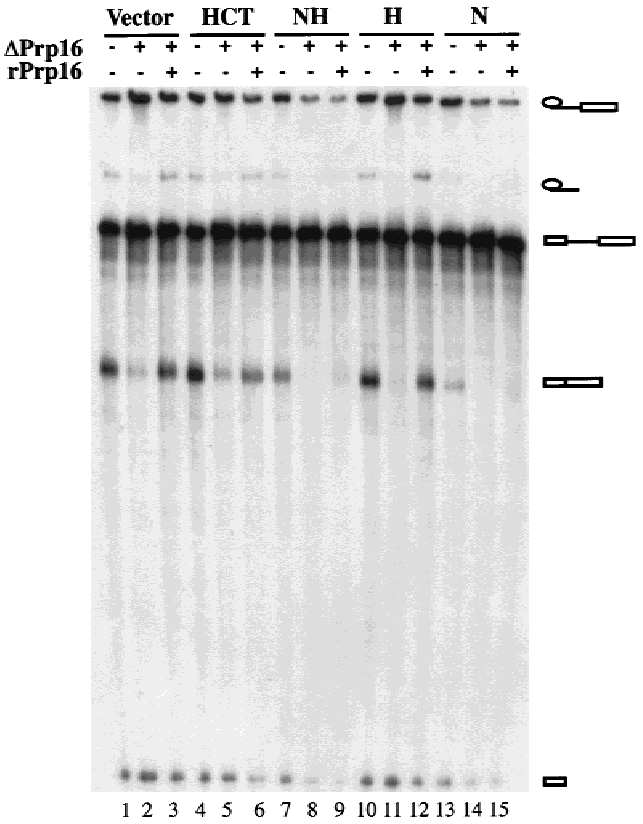

FIGURE 5. Truncations containing the N domain inhibit the function of the wild-type Prp16 protein in vitro. Lanes 1, 4, 7, 10, and 13, splicing of the actin precursor in extract prior to depletion of the wild-type Prp16 protein; lanes 2, 5, 8, 11, and 14, splicing in ΔPrp16 extract for 15 min and continued for 10 min after the addition of buffer only. Lanes 3, 6, 9, 12, and 15, splicing in ΔPrp16 extract for 15 min and continued for 10 min after the addition of ~40 pg of recombinant Prp16. Truncations present in the extract are indicated above the gel.

Prp16 was added to the ΔPrp16 extracts, splicing was fully rescued with extract expressing the H domain (Fig. 5, compare lanes 10 and 12) and with the control extract (Fig. 5, compare lanes 1 and 3). In contrast, no rescue was observed with extract containing NH (Fig. 5, compare lanes 7 and 9) or N (Fig. 5, compare lanes 13 and 15), indicative of an inhibitory effect on the function of the wild-type protein. Although the HCT does not associate with the lariat intermediate based on the co-IP experiment described in the previous section, an inhibition of the rescue is observed with the HCT extract (Fig. 5, compare lanes 4 and 6). Results discussed in the previous section suggest that possible weak interactions between the CT domain and the spliceosome may exist. Such interactions, which may not be stable enough to allow the co-precipitation of splicing intermediates, could interfere with the wild-type function in this more sensitive assay. The fact that the starting HCT extract did not show a splicing defect (Fig. 5, lane 4) suggests that the inhibitory effect of HCT is weaker compared to that of N and NH, and is dependent on the order of addition. Because no trun-

cations can be co-immunoprecipitated with Prp16-HA_3 using the anti-HA antibodies (Y. Wang & C. Guthrie, unpubl. data), the observed inhibition of the wild-type function by the truncations is likely to be achieved by a direct competition on the spliceosome, rather than by sequestering the wild-type protein in solution.

We note that the level of the lariat intermediates is reduced specifically in extract containing either N or NH, especially upon immunodepletion of the full-length Prp16. This observation could be due to either an inhibitory effect of the truncations on the efficiency of the first step of splicing, or a stimulatory effect on the degradation of lariat intermediates. Because no corresponding increase in the precursor level was observed in these two extracts compared to the others, the former possibility is unlikely. Previous studies have implicated Prp16 in a proofreading pathway that allows the degradation of aberrantly formed lariat intermediates (Burgess & Guthrie, 1993). Whether the binding of the truncated Prp16 containing N or NH to the spliceosome could predispose normal splicing intermediates to the discard pathway is an intriguing possibility that remains to be investigated. In summary, the dominant negative effect of the truncations on the wild-type function in vitro is consistent with the N domain being the primary spliceosome binding domain of Prp16, and the CT domains as the secondary spliceosome binding domain.

Overexpression of truncations containing the N domain exacerbates the growth phenotype of ts alleles of PRP16

The results described above identify the N domain of Prp16 as the spliceosome binding domain in vitro. If the same holds true in vivo, overexpression of the N or the NH domains is expected to inhibit the wild-type function as well. When truncations were overexpressed in a wild-type strain containing a single copy of the full-length *PRP16* gene, no dominant negative effect was observed (data not shown). However, when the truncation constructs were transformed into a strain that contains a plasmid-borne *ts* allele, *prp16-2* (Vijayraghavan et al., 1989) (strain YS78-2), *prp16-201* (strain YS78-201), or *prp16-202* (strain YS78-202) (Burgess, 1993) in the *PRP16* deletion background, exacerbation of the *ts* growth phenotype was observed with N and NH domains (Fig. 6, panels 3 and 4), but not with the vector control, the H, or the HCT truncation (Fig. 6, panels 1, 5, and 6). Surprisingly, the *ts* phenotype of each allele was fully suppressed with HCT as with the wild-type PRP16 (Fig. 6, panels 2 and 6). This result was unexpected because this truncation is mislocalized to the cytoplasm. A possible explanation is that HCT may form a complex with the mutant proteins, such that suppression is achieved by *trans*-complementation. This possibility is explored further in the next section.

Why was the dominant negative effect observed only in the mutant *PRP16* strains and not in the wild-type strain? A plausible explanation is that, as observed in the co-IP experiment, the binding affinity of the N or the NH domains for the spliceosome in vivo is reduced compared to that of the wild-type protein. Therefore, the N or the NH domains cannot effectively compete with the wild-type protein in vivo to confer a dominant negative phenotype. However, in the context of the mutant Prp16 proteins, which may be partially defective in binding to the spliceosome at the nonpermissive temperature, the N or NH domains can confer a dominant negative phenotype against these weaker competitors. The fact that overexpression of *prp16-2*, *prp16-201*, and *prp16-202* suppresses their own *ts* phenotype is consistent with a partial defect in spliceosome binding of the mutant proteins, due to either reduced stability or reduced binding affinity.

In summary, the combined in vitro and in vivo approaches allowed us to identify the nonconserved N domain of Prp16 as the primary spliceosome binding domain. Although the CT domains alone cannot stably associate with the spliceosome, their presence does appear to enhance the interactions between the N domain and the spliceosome and maximizes the binding affinity of the full-length protein to the spliceosome.

N and HCT domains can function *in trans* in vivo and in vitro

The function of Prp16 in splicing is dependent on its ability to hydrolyze NTP. It has been shown that a conformational change in the spliceosome occurs upon hydrolysis of NTP by Prp16 (Schwer & Guthrie, 1992a; Umen & Guthrie, 1995a, 1995b). Although the N domain alone can bind to the spliceosome, it is not expected to undergo the ATP-dependent conformational change because of lacking the ATP binding/hydrolysis domain. Therefore, the function of the N domain must be coupled to the function of the HCT domain in order to achieve both the initial association to the spliceosome, which is ATP-independent, and the subsequent ATP-dependent conformational change. Because HCT can complement the *ts* phenotype conferred by *prp16-2*, *prp16-201*, and *prp16-202*, we tested whether *trans*-complementation can be achieved by co-expressing the N and the HCT domains. As shown in Table 2, the deletion of the wild-type *PRP16* is fully complemented by N and HCT that are expressed *in trans*. Furthermore, the extract made from the cells co-expressing the two domains is also functional in complementing the second step of splicing in vitro (data not shown).

Because HCT is mislocalized to the cytoplasm and unable to associate stably with the spliceosome, the *trans*-complementation is unlikely to be achieved by independent binding of the two domains to the spliceosome. A more plausible possibility is that N and HCT

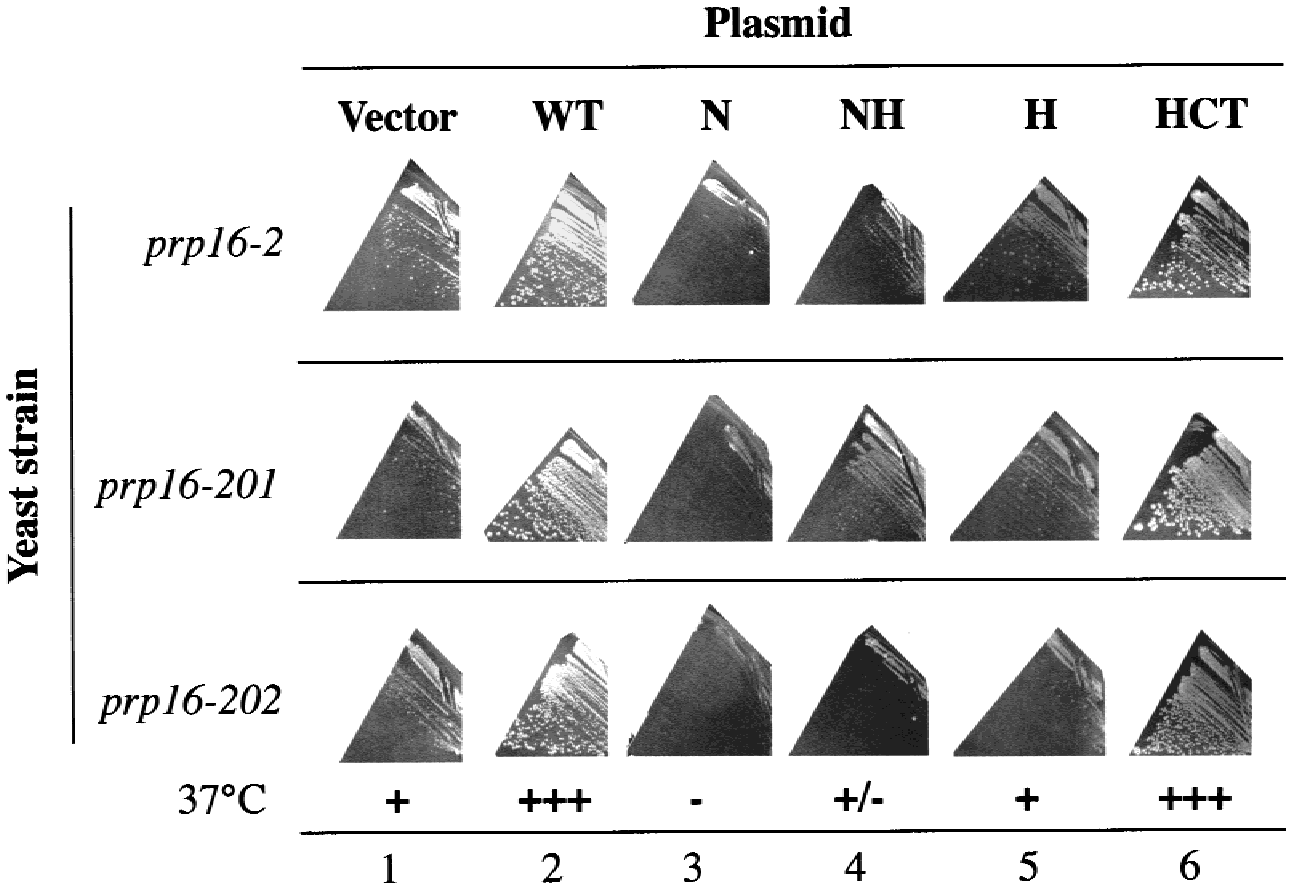

FIGURE 6. Effect of overexpression of truncated Prp16 on the growth phenotype of ts alleles of *PRP16*. A high copy plasmid carrying the individual *PRP16* truncations and under the control of GPD promoter was transformed into yeast strains indicated on the left. A single transformant grown at 25 °C on a media lacking tryptophan was streaked onto the same media and incubated at 37 °C. A plasmid containing just the vector backbone was used as the negative control (Vector; panel 1). A plasmid carrying the wild-type *PRP16* was used as the positive control (WT, panel 2). Growth phenotypes of cells overexpressing truncations were shown (N, panel 3; NH, panel 4; H, panel 5; and HCT, panel 6). The growth phenotype was scored based on the relative size of the colonies: $+++$, similar to the positive control; $+$, similar to the negative control; $+/-$, colonies were smaller than those in the negative control; $-$, no visible colonies.

associate in solution to form a bipartite Prp16, which then functions in splicing. To test this directly, we prepared extract from cells co-expressing HCT-HA_3 and the untagged N domain. The monoclonal anti-HA antibody 12CA5 was then used to immunoprecipitate HCT-HA_3. The immunoprecipitation pellet was checked for the presence of the N domain by immunoblotting using the polyclonal anti-Prp16 antibodies (see Materials and Methods). The untagged N domain was specifically and efficiently co-precipitated along with HCT-HA_3 (Fig. 7, lane 6), consistent with the model that these two regions of Prp16 can interact in solution to form a bipartite protein.

To identify the regions required for *trans*-complementation, we have examined the effect of deletions in the N domain. As shown in Table 2, it is the C-terminal half of the N domain that is essential for *trans*-complementation. Thus, the same region of the N domain that is required for the in vivo function of Prp16 is also necessary and sufficient for *trans*-complementation. Taken together, the finding that N and HCT can function *in trans* strongly suggests that they are structurally separable modules that perform distinct and complementary functions.

DISCUSSION

In this report, we have established the functional importance of the nonconserved N-terminal domain of Prp16 in cell viability, in the localization of the protein to the nucleus, and, most importantly, in mediating specific interactions between Prp16 and the spliceosome. Because the association of Prp16 with the spliceosome is thought to be temporally coupled to its specific function in the second step of splicing, the N domain must play a key role in localizing Prp16 to the site of its action during splicing. The CT domains of Prp16 appear to play an accessory role in stabilizing the binding interactions between the N domain and the spliceosome. Our finding that the N and the HCT domains of

TABLE 2. The N and the HCT domains can function *in trans*.

Plasmid A[a] (CEN, *TRP*)	Plasmid B[b] (2 μ, *HIS*)	Growth on 5-FOA plate[a] 18 °C	25 °C	30 °C	37 °C
Vector	WT PRP16	+++	+++	+++	+++
Vector	HCT	–	–	–	–
N (299 aa)	HCT	+++	+++	+++	+++
N1 (222 aa)	HCT	+++	+++	+++	+++
N2 (151 aa)	HCT	+++	+++	+++	++
N3 (72 aa)	HCT	–	–	–	–

[a]Truncations on plasmid A is under the control of the endogenous *PRP16* promoter.
[b]Truncation on plasmid B is under the control of the GPD promoter.
[c]Single transformant from a −Trp/−His plate was streaked on a preincubated 5-FOA plate and incubated for 4 days at 25, 30, or 37 °C, and for 8 days at 18 °C before scoring.

Prp16 can function *in trans* demonstrates that these two regions function as modules that are structurally separable, physically interacting, and functionally coupled.

Recently, Prp16, Prp22, and U5^{200}, the human homologue of Brr2, have been shown to catalyze RNA duplex unwinding in vitro (Laggerbauer et al., 1998; Schwer & Gross, 1998; Wagner et al., 1998; Wang et al., 1998). However, the unwinding activity of these proteins does not require specific sequences in the RNA substrate (Wagner et al., 1998; Wang et al., 1998), raising the question of how the unwinding substrate of each protein is determined during splicing. Our findings suggest that the spliceosomal targets of the unwinding activity of these proteins are not determined by specific RNA–protein interactions involving the highly conserved DExD/DExH-box domain; rather, we propose that this specificity is determined by interactions between the nonconserved regions in these proteins and other spliceosomal component(s), protein, or RNA (Fig. 8). Once integrated into the spliceosome, the unwinding activity of the DExD/DExH-box protein can target an RNA duplex in its vicinity.

The specific interactions that occur between the nonconserved regions and the spliceosome are likely to be unique for each of the DExD/DExH-box splicing factors. For example, Brr2 or U5^{200}, as an integral component of the U5 snRNP, is recruited into the spliceosome along with the U4/U6.U5 tri-snRNP (Lauber et al., 1996). This protein is thus likely to interact specifically with proteins and/or snRNAs within the tri-snRNP. Intriguingly, Brr2 has been shown recently to be required for the dissociation of the U4/U6 duplex in a multi-snRNP complex (Raghunathan & Guthrie, 1998). For the transiently associating DExD/DExH-box proteins, the specific interactions are most likely to occur at the step of spliceosome binding. The binding of Prp2 to the spliceosome has been shown to be dependent on specific protein–protein interactions with an accessory factor, Spp2 (Roy et al., 1995). In the case of Prp22, the presence of a conserved RNA binding motif (S1, see Fig. 1) in the N domain (Company et al., 1991; Bycroft et al., 1997) points to the possibility that specific protein–RNA interactions may be important for the binding of Prp22 to the spliceosome.

In the case of Prp16, neither an accessory factor nor any known RNA binding motifs have been identified. There are a number of other protein factors, Prp17, Prp18, Slu7, and Prp22, that also function in the second step of splicing. However, because these factors

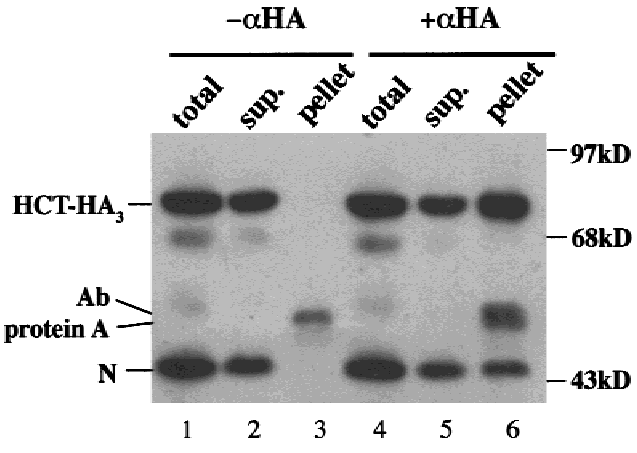

FIGURE 7. The N and the HCT domains can be co-immunoprecipitated. Extract containing HCT-HA$_3$ and untagged N was incubated with antibody 12CA5 bound to the protein-A–sepharose in the presence of 50 mM KCl. The supernatant and pellet are compared along the side of the total input extract. Incubation with the protein-A–sepharose alone was used as the negative control. The protein molecular weight markers are indicated on the right of the gel, and the identities of the bands are indicated at the center. Lanes 1 and 4, total input of extract; lanes 2 and 5, the supernatant from the immunoprecipitation sample; lanes 3 and 6, the pellet from the immunoprecipitation sample; lanes 1–3, no antibody added; lanes 4–6, with antibody 12CA5 added.

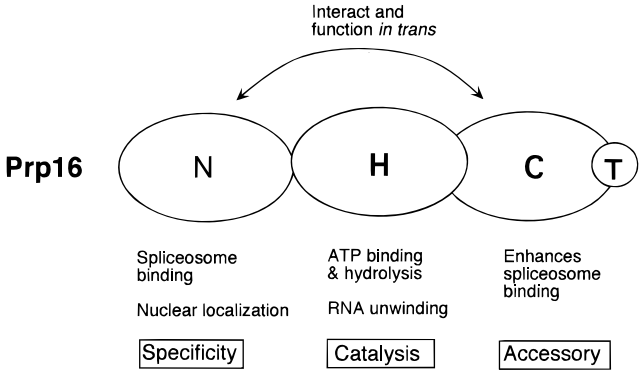

FIGURE 8. Schematic summary of the structure and function correlation in Prp16. The four structural domains (N, H, C, and T; see Fig. 1 for definition) and their corresponding functions are shown. The observed interaction between the N and the HCT domains is indicated at the top.

are conditionally dispensable for splicing either in vivo or in vitro (Horowitz & Abelson, 1993a, 1993b; Ansari & Schwer, 1995; Jones et al., 1995; Brys & Schwer, 1996), they are unlikely to participate in the recruitment of Prp16, which is essential both in vivo and in vitro. Alternatively, the N domain of Prp16 may bind RNA directly during the initial association with the spliceosome. The 3′ splice site of the actin pre-mRNA has been shown to interact with Prp16 by UV crosslinking (Umen & Guthrie, 1995a). However, this interaction is not required for the association of Prp16 with the spliceosome (Brys & Schwer, 1996). Genetic analyses have revealed that a single nucleotide deletion in a region of U6 snRNA can suppress the dominant cold-sensitive phenotype conferred by several *prp16* alleles (Madhani & Guthrie, 1994b), suggesting a possible role of U6 snRNA in interacting with Prp16 on the spliceosome. Further investigation of the mechanism of the N domain-mediated recruitment of Prp16 by the spliceosome will help elucidate the spliceosomal target of the unwinding activity of Prp16.

Mammalian homologues (see Fig. 1) of a number of the yeast DExD/DExH-box splicing factors have been identified, suggesting that the function of these proteins is conserved (Ono et al., 1994; Gee et al., 1997; Laggerbauer et al., 1998; Teigelkamp et al., 1998; Zhou & Reed, 1998). Interestingly, a motif rich in Arg-Ser (RS) dipeptide is present in the N-terminal domain of three mammalian homologues, hPrp16, U5^{100}, and HRH1 (Ono et al., 1994; Teigelkamp et al., 1998; Zhou & Reed, 1998). This motif has been implicated in protein–protein interactions involving SR proteins (Fu, 1995; Manley & Tacke, 1996). In HRH1, the mammalian homologue of Prp22, this motif has been shown to mediate interactions of HRH1 with other SR proteins (Ono et al., 1994). Moreover, deletion of this motif appears to alleviate the dominant negative phenotypes conferred by a mutant allele of HRH1, consistent with its role in spliceosome binding (Ohno & Shimura, 1996). However, it remains to be addressed whether this motif alone is capable of binding to the spliceosome, or simply enhances the binding interactions or regulates the binding interactions through phosphorylation/dephosphorylation of the RS motifs (Xiao & Manley, 1997). The fact that this RS-rich motif is not conserved from yeast to mammals also suggests that, although the catalytic function of these proteins is conserved, the specific interactions involving the N-terminal domain or other nonconserved domains of the protein may well differ. In support of this view, whereas the full-length human Prp16 (hPrp16) cannot substitute for yeast Prp16, a chimeric protein with the N-terminal domain of yeast Prp16 fused to the HCT domains of hPrp16 has been shown to complement the chromosomal deletion of the yeast PRP16 gene (Zhou & Reed, 1998).

Recently, the three-dimensional structures of PcrA and Rep, members of the helicase superfamily I (SF I), and truncated HCV NS3 RNA helicase, a SF II member, have been solved (Subrananya et al., 1996; Kim et al., 1997; Korolev et al., 1997; Yao et al., 1997). Notably, the nonconserved regions of these proteins form independent structural domains from the conserved regions. Despite distinct functional specificity, striking structural similarity is found among the helicase domains and the core structure of the recA protein (Subrananya et al., 1996; Bird et al., 1998; Korolev et al., 1998; Staley & Guthrie, 1998). It has been proposed that the mechanism of signaling between ATP binding/hydrolysis and protein conformational change may be similar in each of these ATPases (Subrananya et al., 1996). The structural details of the helicase domain are likely to be conserved in other members of both helicase superfamilies. In contrast, the nonconserved regions are likely to be structurally distinct, and to couple the nonspecific ATPase/helicase activity to a specific step or process by interacting with other proteins and/or nucleic acids. This strategy can readily account for the functional diversity exhibited by the DExD/DExH-box protein family and the helicases in general. In addition to bringing the catalytic activity to its target, the nonconserved regions might also regulate (positively or negatively) the ATPase and/or helicase activities. The answers to these intriguing questions are important goals for the future.

MATERIALS AND METHODS

Materials

Restriction enzymes were purchased from New England Biolabs; T4 DNA ligase and DNA Sequenase, from U.S. Biochemical; 5-FOA, from PCR Incorporated; Hot Tub DNA polymerase and ECL western blot reagent, from Amersham Life Science; polyacrylamide chromatography materials, from Whatman and Pharmacia. Oligonucleotides were synthesized by H. Madhani and Y. Wang on a Milligene DNA synthesizer. Protein gel and electroblotting apparatus were from Bio-Rad.

Strains

The following *S. cerevisiae* strains were used in this study. YS78: *Mata trp1 ura3 his3 lys2 leu2 ade2 prp16Δ::LYS2*, pSB2 (*PRP16 URA3*) (constructed by S. Burgess); YS78-2: pSB2 in YS78 is replaced by p62-2 (*prp16-2 HIS3*); YS78-201: pSB2 in YS78 is replaced by p62-201 (*prp16-201 HIS3*); YS78-202: pSB2 in YS78 is replaced by p62-202 (*prp16-202 HIS3*).

Plasmids

Standard cloning procedures were used in the construction of the following plasmids. pSE358 and pSE362 were constructed and provided by Steve Ellege. They contain yeast *ARSI*, *CEN4*, and *TRP1* or *HIS3*, and Amp^r for selection in

Escherichia coli. pG-1 was constructed by Schena et al. (1991). It contains yeast *TRP1* gene and 2-μm origin of replication and the Amp^r gene. pYWI58 was constructed by first inserting the *Eco*R I/*Sph* I fragment of pSB58 (Burgess & Guthrie, 1993) into the polylinker on pSE358, and then replacing the *Kpn* I/*Kpn* I fragment with that of pSphHKIN (from Beate Schwer), which contains the *Nde* I site at the +1 position of the *PRP16* ORF. pYWII was constructed by inserting linker HSAC into pG-1 at the *Bam*H I/*Sal* I site to introduce a region encoding a His_6 tag.

Deletion of the N domain

pYWI-HCT was constructed by replacing the *Nde* I/*Xho* I fragment of pYWI with linker NX. pYWIΔN1, pYWIΔN2, and pYWIΔN3 were constructed by replacing the *Nde* I/*Xho* I fragment of pYWI with the PCR fragments generated using primers ΔN1/ΔNXho, ΔN2/ΔNXho, and ΔN3/ΔNXho, respectively. p62ΔN3 was constructed by inserting the *Eco*R I/*Sal* I fragment of pYWIΔN3 into pSE362.

Deletion of the T domain

pYW18 was constructed by inserting the *Xba* I/*Sph* I fragment of pSB58 into the polylinker of pUC18; pYW18ΔT was constructed by replacing the *Bcl* I/*Sph* I fragment of pYW18 with the linker TSC; p58ΔT was constructed by replacing the *Spe* I/*Sph* I fragment of pSB58 with that of pYW18ΔT.

Deletion of both the N and T domains

pYWIΔN1T, pYWΔN2T, and pYWΔN3T were constructed by replacing the *Nde* I/*Xho* I fragment of pYWΔT with the same restriction fragment from pYWIΔN1, pYWΔN2, and pYWΔN3, respectively.

Deletion of the CT domains

The *Eco*R I/*Sal* I fragment of pYWI was inserted into pUC18 to construct pYW18RS. The *Cla* I/*Eco*R V fragment of pYW18RS was deleted to generate plasmid pYW18NH. pYWINH was constructed by inserting the *Eco*R I/*Sal* I fragment of pYW18NH into the polylinker of pSE358.

Deletion of multiple domains

pYWI-H was constructed by replacing the *Nde* I/*Xho* I fragment of pYWINH with linker NX. pYWICT was constructed by deleting the *Xho* I/*Cla* I fragment of pYWI-HCT followed by Klenow fill-in and ligation. pYWIN was constructed by first making pYW18N by deleting the *Xho* I/*Eco*R V fragment of pYW18RS followed by Klenow fill-in and ligation, and then replacing the *Nde* I/*Sal* I fragment of pYWI with that of pYW18N.

Chimera 2N16

A PCR fragment was generated using a plasmid carrying the PRP2 gene as the template and DNA oligonucleotides P2-N and P2-X1 as the primers. The resulting fragment contained the coding region for amino acid 1–200 of Prp2 protein and flanked by an *Nde* I site at the 5′ end and a *Xho* I site at the 3′ end. This fragment was then inserted into pYWI58N after digestion with *Nde* I and *Xho* I. The high copy construct of this chimera was made as described below.

High copy constructs

All high copy plasmids (pYWII series) were constructed by inserting the *Nde* I/*Sal* I fragment from the corresponding low copy plasmid (pYWI series) into pYWII at the *Sac* I/*Sal* I sites. All high copy constructs express a polypeptide with a His_6-tag at the N terminus.

HA_3-tagged constructs

The DNA encoding the triple HA tag was amplified by PCR using primers HASS1 and HASS2. The resulting PCR fragment was first subjected to *Sac* I and *Sal* I digestions and then inserted into the *Sac* I/*Sal* I sites of YWI58 to make the construct expressing Prp16-HA_3, and into the same sites of YWIIΔN to make HCT-HA_3. The same method was used to make 2N16-HA_3. The successful insertion of the tag was confirmed by western analysis using the 12CA5 monoclonal antibody.

DNA oligonucleotides

Linkers

HSAC	5′-CATATGCACCACCATCACCATCACGGAGCTC GCG-3′
	3′-GTATACGTGGTGGTTGAGGTTGAGCCTCGA GCACGGCT-5′
NX	5′-TATGGGTCAATC-3′
	3′-ACCCAGTTAGAGCT-5′
TSC	5′-GATCCGTAGATAAGTAAGGCATG-3′
	3′-GCATCTATTCATTCC-5′

PCR primers (5′ → 3′)

ΔN1	GGAATTCCATATGTCGACAGGCCCAAAGAAAAT
ΔN2	GGAATTCCATATGACACAGAATGGTCATGCTG
ΔN3	GGAATTCCATATGATCCCTCCTTTTTTATCAAAG
ΔNxho	GCCGCTCGAGATTGTTGAATATGTTC
HASS1	CGCGAGCTCGGCCGCATCTTTTACCC
HASS2	GCGCGTCGACCTAGCACTGAGCAGCGTAATC
$P_{2\text{-}N}$	CCCCATATGTCAAGTATTACATCTGAA
$P_{2\text{-}X1}$	CCCTCGAGCCTCATATTGAAGTTTCTC

ECL western analysis

Liquid culture of 5 mL was allowed to grow to $OD_{600nm} = 1$ before harvest. The cell pellet was resuspended in 500 μL ice-cold TCA buffer (20 mM Tris-HCl, pH 8, 50 mM ammonium acetate, and 2 mM EDTA) with 2× protease inhibitor cocktail (0.2 mg/mL PMSF, 2 mM benzamide, 2 μg/mL leupeptin, and 2 μg/mL of trasylol), and mixed with 100 μL acid-washed glass beads and 500 μL ice-cold 20% TCA. The

cells were lysed by vortexing twice for 30 s. The supernatant was transferred to a new tube and centrifuged for 10 min at 4 °C. The pellet was resuspended in 300 μl loading buffer (120 mM Tris base, 3.5% SDS, 8 mM EDTA, 14% glycerol, and 120 mM DTT) and analyzed on SDS-PAGE after heating at 95 °C for 10 min. Following electrophoresis, the proteins were transferred onto a nitrocellulose membrane using Bio-Rad electroblotter at 30 V for 3 h at 4 °C. The western blotting was performed using the polyclonal anti-Prp16 antibodies (Schwer & Guthrie, 1991) as the primary antibody and the HRP-conjugated goat-anti-rabbit antibody (Amersham) as the secondary antibody.

Immunofluorescence

Cells were first grown to OD_{600nm} = 0.15 in media selecting for the plasmid expressing the tagged protein. Cells were collected by low-speed centrifugation (<3,000 rpm) and diluted into YPD to OD_{600nm} = 0.1, and allowed to grow to OD_{600nm} = 0.2. One milliliter of the culture was mixed with 135 μL 37% formaldehyde (Fluka) and fixed for 1 h. Fixed cells were washed with sorbital buffer and were spheroplasted with zymolyase (40 μg/mL). Slides were pretreated with 1 mg/mL polylysine (Sigma) before applying the cells to improve cell adhesion. Blocking buffer (Boehringer Mannheim) was added to prevent nonspecific protein binding. Binding of the fluorochrome was achieved by first incubating with the primary antibody 12CA5 (1:150 dilution), followed by an incubation with the fluorescein isothiocyanate (FITC)-conjugated goat anti-mouse antibody. Staining with 4′,6-diamidino-2-phenylindole (DAPI) was achieved by including DAPI in the mounting solution. The immunofluorescence analyses were done using a Zeiss Axioskop microscope with a 100-W mercury lamp and a plan-neofluor 100 (N.A. 1.3).

Preparation of splicing extract and immunodepletion of Prp16

Splicing extracts were prepared as previously reported (Umen & Guthrie, 1995a) with the following modification. Cells were grown to OD_{600nm} = 1.0 in selective media before diluting into YPD media to OD_{600nm} = 0.25, and allowed to grow to OD_{600nm} = 2.0–2.5. Cells were ground to a fine powder using a mortar on dry ice and with the addition of liquid nitrogen. The cell powder was then thawed in a 4 °C water bath. The supernatant collected after 30 min centrifugation at 17,000 rpm was subjected to 80 min ultracentrifugation at 37,000 rpm using a 50Ti rotor. The extract was dialyzed against 2 liters of buffer D [20 mM Hepes-KOH, pH 7.9, 0.2 mM EDTA, 50 mM KCl, 20% (v/v) glycerol, and 0.5 mM DTT] (Umen & Guthrie, 1995a) twice for 1.5 h each time, and stored at −80 °C after quick freezing in liquid nitrogen.

Immunodepletion of Prp16 was performed as reported previously (Schwer & Guthrie, 1991) with minor modifications. One-hundred microliters of extract were incubated with 5 μL (18 mg/mL) protein A purified anti-Prp16 antibodies on ice for 1 h. Pre-equilibrated protein A–sepharose suspension of 50 μL in buffer D was added to the extract–antibody mixture and allowed to incubate with rocking at 4 °C for 1 h. The supernatant was then collected and tested for the efficiency of depletion by in vitro splicing. When necessary, the above immunodepletion procedure was repeated with half of the amount of antibody and protein A–sepharose to increase the efficiency of depletion.

Immunoprecipitation

Immunoprecipitation of the HA_3-tagged proteins was performed as follows. Extract (20 μL) was incubated with 5 μL of 12CA5 antibody (1 mg/mL) on ice for 1 h. Protein A–sepharose suspension of 40 μL and 200 μL of buffer IPP50 (50 mM NaCl in 10 mM Tris-HCl, pH 8.0) were added to the extract–antibody mixture and allowed to incubate with rocking at 4 °C for 30–60 min. The beads were collected by low-speed centrifugation and were washed three times with 200 μL of IPP50. The pellet was boiled in Laemmli gel loading buffer and analyzed on SDS-PAGE by western analyses probed with polyclonal anti-Prp16 antibodies.

Immunoprecipitation using the polyclonal anti-Prp16 antibodies under splicing conditions was done as previously reported (Schwer & Guthrie, 1991; Umen & Guthrie, 1995a) with some modifications. Excess cold actin precursor was added to the splicing reaction prior to the addition of the antibody–protein A sepharose mixture to minimize the nonspecific binding of proteins to the labeled precursor. Non-ionic detergent (NP40) of 0.1% was included or omitted from the immunoprecipitation buffer as indicated in individual experiments.

Expression of recombinant Prp16 in *E. coli*

The 3-kb *Nde* I/*Sal* I fragment, containing the region encoding the His_6-tagged Prp16, from pYWII58 was subcloned into a T7 overexpression vector, pET11a. This plasmid, pYWIII58, was transformed into BL21DE3 (Lys S) strain. A fresh single colony from the LB plate containing ampicillin (100 μg/mL) and chloramphenicol (40 μg/mL) was used to inoculate 10 mL M9LB (IXM9, 0.4% glucose and 1 mM $MgSO_4$ in LB), and allowed to grow at 37 °C to OD_{600nm} = 0.4–0.8, and stored at 4 °C overnight. The overnight culture was used to inoculate 2 liters of M9LB supplemented with ampicillin (200 μg/mL) and chloroamphenicol (40 μg/mL) and allowed to grow to OD_{600nm} = 0.2–0.4 at 30 °C before the addition of IPTG (0.75 μM). Cells were harvested 3 h after the induction and washed with 50 mL of TE (10 mM Tris-HCl, pH 7.5, 0.1 mM EDTA). Cell lyses and protein purification were performed as described previously (Wang et al., 1998).

ACKNOWLEDGMENTS

We thank members of the Guthrie laboratory for discussions and suggestions during the course of this work, in particular, Anne de Bruyn Kops for her expert help in the immunofluorescence experiment. We are grateful to Jon Staley, Amy Kistler, Steven Rader, and Cathy Colins for critical reading of the manuscript. This work is supported by NIH grant GM21119 to C.G., Damon Runyon–Walter Winchell postdoctoral fellowship DRG1245 and subsequently American Cancer Society (California Division) postdoctoral fellowship #1-45-96 to Y.W. C.G. is an American Cancer Society Research Professor of Molecular Genetics.

Received June 11, 1998; returned for revision July 6, 1998; revised manuscript received July 22, 1998

REFERENCES

Ansari A, Schwer B. 1995. SLU7 and a novel activity, SSF1, act during the PRP16-dependent step of yeast pre-mRNA splicing. *EMBO J 14*:4001–4009.

Arenas J, Abelson J. 1997. Prp43: A novel RNA helicase-like factor involved in spliceosome disassembly. *Proc Natl Acad Sci USA 94*:11798–11802.

Ares MJ, Weiser B. 1995. Rearrangement of snRNA structure during assembly and function of the spliceosome. *Prog Nucleic Acid Res Mol Biol 50*:131–159.

Bird LE, Subramanya HS, Wigley DB. 1998. Helicases: A unifying structural theme? *Curr Opin Struct Biol 8*:14–18.

Brys A, Schwer B. 1996. Requirement for SLU7 in yeast pre-mRNA splicing is dictated by the distance between the branchpoint and the 3′ splice site. *RNA 2*:707–717.

Burgess SM. 1993. *Control of mRNA splicing fidelity by the RNA dependent ATPase Prp16* [thesis]. San Francisco, California: University of California.

Burgess SM, Guthrie C. 1990. A putative ATP binding protein influences the fidelity of branchpoint recognition in yeast splicing. *Cell 60*:705–717.

Burgess SM, Guthrie C. 1993. A mechanism to enhance mRNA splicing fidelity: The RNA-dependent ATPase Prp16 governs usage of a discard pathway for aberrant lariat intermediates. *Cell 73*:1377-1391.

Bycroft M, Hubbard TJ, Proctor M, Freund SM, Murzin AG. 1997. The solution structure of the S1 RNA binding domain: A member of an ancient nucleic acid-binding fold. *Cell 88*:235–242.

Chen JH, Lin RJ. 1990. The yeast PRP2 protein, a putative RNA-dependent ATPase, shares extensive sequence homology with two other pre-mRNA splicing factors. *Nucleic Acids Res 18*:6447.

Company M, Arenas J, Abelson J. 1991. Requirement of the RNA helicase-like protein PRP22 for release of messenger RNA from spliceosomes. *Nature 349*:487–493.

Dalbadie-McFarland G, Abelson J. 1990. PRP5: A helicase-like protein required for mRNA splicing in yeast. *Proc Natl Acad Sci USA 87*:4236–4240.

Fu X. 1995. The superfamily of arginine/serine-rich splicing factors. *RNA 1*:663–680.

Fuller-Pace FV. 1994. RNA helicases: Modulators of RNA structure. *Trends Cell Biol 4*:271–274.

Gee S, Krauss SW, Miller E, Aoyagi K, Arenas J, Conboy JG. 1997. Cloning of mDEAH9, a putative RNA helicase and mammalian homologue of *Saccharomyces cerevisiae* splicing factor Prp43. *Proc Natl Acad Sci USA 94*:11803–11807.

Gorbalenya AE, Koonin EV. 1993. Helicases: Amino acid sequence comparisons and structure–function relationships. *Curr Opin Struct Biol 3*:419–429.

Gross CH, Shuman S. 1995. Mutational analysis of vaccinia virus nucleoside triphosphate phosphohydrolase II, a DExH bos RNA helicase. *J Virol 69*:4727–4736.

Guthrie C. 1991. Messenger RNA splicing in yeast: Clues to why the spliceosome is a ribonucleoprotein. *Science 253*:157–163.

Horowitz D, Abelson J. 1993a. Stages in the second reaction of pre-mRNA splicing: The final step is ATP independent. *Genes & Dev 7*:320–329.

Horowitz DS, Abelson J. 1993b. A U5 small nuclear ribonucleoprotein particle protein involved only in the second step of pre-mRNA splicing in *Saccharomyces cerevisiae*. *Mol Cell Biol 13*:2959–2970.

Hotz H, Schwer B. 1998. Mutational analysis of the yeast DEAH-box splicing factor Prp16. *Genetics*. Forthcoming.

Jones M, Frank D, Guthrie C. 1995. Characterization and functional ordering of Slu7p and Prp17p during the second step of pre-mRNA splicing in yeast. *Proc Natl Acad Sci USA 92*:9687–9691.

Kim JL, Morgenstern KA, Griffith JP, Dwyer MD, Thomson JA, Murcko MA, Lin C, Caron PR. 1997. Hepatitis C virus NS3 RNA helicase domain with a bound oligonucleotide: The crystal structure provides insights into the mode of unwinding. *Structure 6*:89–100.

Kim SH, Smith J, Claude A, Lin RJ. 1992. The purified yeast pre-mRNA splicing factor PRP2 is an RNA-dependent NTPase. *EMBO J 11*:2319–2326.

Korolev S, Hsieh J, Gauss GH, Lohman TM, Waksman G. 1997. Major domain swiveling revealed by the crystal structures of complexes of *E. coli* Rep helicase bound to single stranded DNA and ADP. *Cell 90*:635–647.

Korolev S, Yao N, Lohman TM, Weber PC, Waksman G. 1998. Comparisons between the structures of HCV and Rep helicases reveal structural similarities between SF1 and SF2 super-families of helicases. *Protein Sci 7*:605–610.

Laggerbauer B, Achsel T, Lührmann R. 1998. The human 200kD DEXH-box U5 snRNP protein unwinds U4/U6 RNA duplices in vitro. *Proc Natl Acad Sci USA 95*:4188–4192.

Lauber J, Fabrizio P, Teigelkamp S, Lane W, Hartmann E, Lührmann R. 1996. The HeLa 200 kDa U5 snRNP-specific protein and its homologue in *Saccharomyces cerevisiae* are members of the DEXH-box protein family of putative RNA helicases. *EMBO J 15*:4001–4015.

Lin J, Rossi JJ. 1996. Identification and characterization of yeast mutants that overcome an experimentally introduced block to splicing at the 3′ splice site. *RNA 2*:835–848.

Lin RJ, Newman AJ, Cheng SC, Abelson J. 1985. Yeast mRNA splicing in vitro. *J Biol Chem 260*:14780–14792.

Madhani HD, Guthrie C. 1994a. Dynamic RNA–RNA interactions in the spliceosome. *Annu Rev Genet 28*:1–26.

Madhani HD, Guthrie C. 1994b. Genetic interactions between the yeast RNA helicase homolog Prp16 and spliceosomal snRNAs identify candidate ligands for the Prp16 RNA-dependent ATPase. *Genetics 137*:677–687.

Manley J, Tacke R. 1996. SR proteins and splicing control. *Genes & Dev 10*:1569–1579.

Moore MJ, Query CC, Sharp PA. 1993. Splicing of precursors to mRNA by the spliceosome. In: Gesteland RF, Atkins JF, eds. *The RNA world*. Cold Spring Harbor, New York: Cold Spring Harbor Laboratory Press. pp 303–358.

Nilsen TW. 1998. RNA–RNA interactions in nuclear pre-mRNA splicing. In: Simons R, Grunberg-Manago M, eds. *RNA structure and function*. Cold Spring Harbor, New York: Cold Spring Harbor Laboratory Press. pp 279–307.

Noble SM, Guthrie C. 1996. Identification of novel genes required for yeast pre-mRNA splicing by means of cold-sensitive mutations. *Genetics 143*:67–80.

O'Day CL, Dalbadie-McFarland G, Abelson J. 1996. The *Saccharomyces cerevisiae* Prp5 protein has RNA-dependent ATPase activity with specificity for U2 small nuclear RNA. *J Biol Chem 271*:33261–33267.

Ohno M, Shimura Y. 1996. A human RNA helicase-like protein, HRH1, facilitates nuclear export of spliced mRNA by releasing the RNA from the spliceosome. *Genes & Dev 10*:997–1007.

Ono Y, Ohno M, Shimura Y. 1994. Identification of a putative RNA helicase (HRH1), a human homolog of yeast Prp22. *Mol Cell Biol 14*:7611–7620.

Pause A, Methot N, Sonenberg N. 1993. The HRIGRXXR region of the DEAD box RNA helicase eukaryotic translation initiation factor 4A is required for RNA binding and ATP hydrolysis. *Mol Cell Biol 13*:6789–6798.

Pause A, Sonenberg N. 1992. Mutational analysis of a DEAD box RNA helicase: The mammalian translation initiation factor eIF-4A. *EMBO J 11*:2643–2654.

Raghunathan P, Guthrie C. 1998. RNA unwinding in U4/U6 snRNPs requires ATP hydrolysis and the DEIH-box splicing factor Brr2. *Curr Biol 8*:847–855.

Roy J, Kim K, Maddock JR, Anthony JG, Woolford JLJ. 1995. The final stages of spliceosome maturation require Spp2p that can interact with the DEAH box protein Prp2p and promote step 1 of splicing. *RNA 1*:375–390.

Rozen F, Edery I, Meerovitch K, Dever TE, Merrick WC, Sonenberg N. 1990. Bidirectional RNA helicase activity of eukaryotic translation initiation factors 4A and 4F. *Mol Cell Biol 10*:1134–1144.

Ruby SW, Abelson J. 1991. Pre-mRNA splicing in yeast. *Trends Genet 7*:79–85.

Rymond BC, Rosbash M. 1992. Yeast pre-mRNA splicing. In: Jones EW, Pringle JR, Broach JR, eds. *The molecular and cellular biology of the yeast Saccharomyces*. Cold Spring Harbor, New York: Cold Spring Harbor Laboratory Press. pp 143–182.

Schena M, Picard D, Yamamoto K. 1991. Vectors for constitutive and inducible gene expression in yeast. *Methods Enzymol 194*:389–398.

Schmid SR, Linder P. 1992. D-E-A-D protein family of putative RNA helicase. *Mol Microbiol 6*:283–291.

Schwer B, Gross CH. 1998. Prp22, a DExH-box RNA helicase, plays two distinct roles in yeast pre-mRNA splicing. *EMBO J 17*:2086–2094.

Schwer B, Guthrie C. 1991. PRP16 is an RNA-dependent ATPase that interacts transiently with the spliceosome. *Nature 349*:494–499.

Schwer B, Guthrie C. 1992a. A conformational rearrangement in the spliceosome is dependent on PRP16 and ATP hydrolysis. *EMBO J 11*:5033–5039.

Schwer B, Guthrie C. 1992b. A dominant negative mutation in a spliceosomal ATPase affects ATP hydrolysis but not binding to the spliceosome. *Mol Cell Biol 12*:3540–3547.

Sikorski RS, Boeke JD. 1991. In vitro mutagenesis and plasmid shuffling: From cloned gene to mutant yeast. *Methods Enzymol 194*:302–318.

Staley JP, Guthrie C. 1998. Mechanical devices of the spliceosome: Motors, clocks, springs and things. *Cell 92*:315–326.

Strauss EJ, Guthrie C. 1991. A cold-sensitive mRNA splicing mutant is a member of the RNA helicase gene family. *Genes & Dev 5*:629–641.

Subrananya HS, Bird LE, Brannigan JA, Wigley DB. 1996. Crystal structure of a DExx box DNA helicase. *Nature 384*:379–383.

Teigelkamp S, McGarvey M, Plumpton M, Beggs JD. 1994. The splicing factor PRP2, a putative RNA helicase, interacts directly with pre-mRNA. *EMBO J 13*:888–897.

Teigelkamp S, Mundt C, Achsel T, Will CL, Lührmann R. 1998. The human U5 snRNP-specific 100kD protein is an RS domain containing putative RNA helicase with significant homology to the yeast splicing factor Prp28p. *RNA 3*:1313–1326.

Umen JG, Guthrie C. 1995a. Prp16p, Slu7p, and Prp8p interact with the 3′ splice site in two distinct stages during the second catalytic step of pre-mRNA splicing. *RNA 1*:584–597.

Umen JG, Guthrie C. 1995b. The second catalytic step of pre-mRNA splicing. *RNA 1*:869–885.

Vijayraghavan U, Company M, Abelson J. 1989. Isolation and characterization of pre-mRNA splicing mutants of *Saccharomyces cerevisiae*. *Genes & Dev 3*:1206–1216.

Wagner JDO, Eckhard J, Company M, Pyle AM, Abelson J. 1998. The DEAH-box protein Prp22 is an ATPase that mediates ATP-dependent mRNA release from the spliceosome and unwinds RNA duplexes. *EMBO J*. Forthcoming.

Wang Y, Wagner JDO, Guthrie C. 1998. The DEAH-box splicing factor Prp16 unwinds RNA duplexes in vitro. *Curr Biol 8*:441–451.

Will CL, Lührmann R. 1997. Protein functions in pre-mRNA splicing. *Curr Opin Cell Biol 9*:320–328.

Xiao S, Manley J. 1997. Phosphorylation of the ASF/SF2 RS domain affects both protein–protein and protein–RNA interactions and is necessary for splicing. *Genes & Dev 11*:334–344.

Xu DN, Nouraini S, Field D, Tang SJ, Friesen JD. 1996. An RNA-dependent ATPase associated with U2/U6 snRNAs in pre-mRNA splicing. *Nature 381*:709–713.

Yao N, Hesson T, Cable M, Hong Z, Kwong AD, Le HV, Weber PC. 1997. Structure of the hepatitis C virus RNA helicase domain. *Nature Struct Biol 4*:463–467.

Zhou Z, Reed R. 1998. Human homologs of yeast Prp16 and Prp17 reveal conservation of the mechanism for catalytic step II of pre-mRNA splicing. *EMBO J 17*:2095–2106.